CHEMISTRY OF MATERIALS
Article

Chem. Mater. **2010,** *22,* 4045–4055 4045
DOI:10.1021/cm100877h

Facile Conversion of Electrospun TiO_2 into Titanium Nitride/Oxynitride Fibers

Marketa Zukalova,*[,†] Jan Prochazka,[†] Zdenek Bastl,[†] Jiri Duchoslav,[‡] Lukas Rubacek,[‡] David Havlicek,[§] and Ladislav Kavan*[,†]

[†]*J. Heyrovsky Institute of Physical Chemistry, v.v.i., Academy of Sciences of the Czech Republic, Dolejskova 3, CZ-18223 Prague 8, Czech Republic,* [‡]*Elmarco, s.r.o., V Horkach 76/18, 460 07 Liberec, Czech Republic, and* [§]*Department of Inorganic Chemistry, Faculty of Science, Charles University, Hlavova 2030, CZ-12840 Prague 2, Czech Republic*

Received March 27, 2010. Revised Manuscript Received May 12, 2010

Nanocrystalline fibrous TiO_2 (anatase) was prepared by electrostatic spinning from ethanolic solution of Ti(IV) butoxide, acetylacetone, and poly(vinylpyrrolidone) employing the Nanospider industrial process. These titania fibers were smoothly converted into cubic titanium oxynitride, TiO_xN_y fibers (a = 4.1930 Å) during 4 h at 600 °C in ammonia atmosphere. The obtained material is convertible back into TiO_2 fibers by heat treatment in air at 500 °C. The TiO_2 fibers, which were reformed in this way, contain anatase as the main phase. Their follow-up reaction with NH_3 at 600 °C/2 h leads to a less crystalline oxynitride material with $a \approx 4.173$ Å, which is close to that of cubic TiO. Three subsequent cycles of this transformation were demonstrated. The described conversions are specific for electrospun anatase fibers only. At the same experimental conditions, other forms of nanocrystalline anatase do not react with ammonia yielding cubic phases. An almost perfectly stoichiometric titanium nitride, TiN (a = 4.2290 Å) containing only 0.2 wt % O, was prepared from TiO_xN_y fibers in NH_3 at temperatures up to 1000 °C. This TiN material maintains the morphology of fibers and is composed of nanocrystals of a similar size as those of the precursor.

1. Introduction

Titanium dioxide is a popular photocatalyst, and its nitrogen-doping (e.g., by thermal treatment in NH_3) has been a subject of intense research, triggered by the pioneering work of Asahi et al.[1] The interest has been motivated by the fact that the N 2p states, created by substitutional doping of the O-sites, are located above the valence band edge. Mixing of these states with O 2p causes a decrease in the band gap, which shifts the photocatalytic activity of titania from UV to visible light. Nevertheless, the band gap narrowing in N-doped TiO_2 is far from being consistently interpreted, and various other structures with N, NH_x, or N_2 in substitutional/interstitial positions were considered, too.[2,3] The optimal material for photocatalysis ($TiO_{1.9925}N_{0.0075}$) was synthesized by treating the TiO_2 powder in the NH_3(67%)/Ar atmosphere at 550 to 600 °C.[1] Schmuki et al.[4] studied nitrogen-doping of electrochemically grown TiO_2 nanotubes by annealing them in NH_3 at 300−600 °C. Consistent with other works on nanocrystalline titania[1,2,5] they found $TiO_{2-x}N_x$, anatase, and rutile, but no cubic nitride/oxynitride in the doped nanotubes.[4] Cui et al.[6] reported on a reverse synthetic route, that is, the preparation of visible-light-responsive $TiO_{2-x}N_x$ from the TiN precursor. The TiN → $TiO_{2-x}N_x$ conversion took place in thin films during calcination in air at 350 °C, but unfortunately, the product was not clearly characterized in this work.[6]

Titanium nitride, TiN, and titanium oxynitrides, TiO_xN_y, adopt the rock-salt crystal structure of osbornite. The oxynitrides are considered to be solid solutions of cubic TiN (a = 4.241 Å) and TiO (a = 4.173 to 4.185 Å).[7,8] They are often prepared by chemical vapor deposition and similar techniques in thin films.[8−14] Particularly, the atomic layer deposition from *tetrakis*(dimethylamino)titanium or

*Corresponding author. E-mail: zukalova@jh-inst.cas.cz (M.Z.); kavan@jh-inst.cas.cz (L.K.).

(1) Asahi, R.; Morikawa, T.; Ohwaki, T.; Aoki, K.; Taga, Y. *Science* **2001**, *293*, 269.
(2) Mi, L.; Xu, P.; Wang, P. N. *Appl. Surf. Sci.* **2008**, *255*, 2574.
(3) Cong, Y.; Zhang, J.; Chen, F.; Anpo, M. *J. Phys. Chem. C* **2007**, *111*, 6976.
(4) Vitiello, R. P.; Macak, J. M.; Ghicov, A.; Tsuchiya, H.; Dick, L. F. P.; Schmuki, P. *Electrochem. Commun.* **2006**, *8*, 544.
(5) Kosowska, B.; Mozia, S.; Morawski, A. W.; Grzmil, B.; Janus, M.; Kalucki, K. *Sol. Energy Mat. Sol. Cells* **2005**, *88*, 269.
(6) Cui, X.; Ma, M.; Zhang, W.; Yang, Y.; Zhang, Z. *Electrochem. Commun.* **2008**, *10*, 367.
(7) Yang, X.; Li, C.; Yang, B.; Wang, W.; Qiam, Y. *Chem. Phys. Lett.* **2004**, *383*, 502.
(8) Drygas, M.; Czosnek, C.; Paine, R. T.; Janik, J. F. *Chem. Mater.* **2006**, *18*, 3122.
(9) Rizzo, A.; Signore, M. A.; Mirenghi, L.; Luccio, T. D. *Thin Solid Films* **2009**, *517*, 5956.
(10) Chan, M. H.; Lu, F. H. *Thin Solid Films* **2009**, *517*, 5006.
(11) Trenczek-Zajac, A.; Radecka, M.; Zakrzewska, K.; Brudnik, A.; Kusior, E.; Bourgeois, S.; Marco De Lucas, M. C.; Imhoff, L. *J. Power Sources* **2009**, *194*, 93.
(12) Song, X.; Gopireddy, D.; Takoudis, C. G. *Thin Solid Films* **2008**, *516*, 6330.
(13) Musschoot, J.; Xie, Q.; Deduytsche, D.; Ven den Berghe, S.; Meirhaeghe, R. L.; Detavernier, C. *Microelectron. Eng.* **2009**, *86*, 72.
(14) Caubet, P.; Blomberg, T.; Benabound, R.; Wyon, C.; Blanquet, E.; Gonchond, J. P.; Juhel, M.; Bouvet, P.; Gros-Jean, M.; Michailos, J.; Richard, C.; Iteprat, B. *J. Electrochem. Soc.* **2008**, *155*, H625–H632.

Published on Web 06/02/2010

tetrakis(diethylamino)titanium (with or without NH_3 as coreactant) produces high-quality TiN films at low temperatures.[13,14] TiN finds broad use for coatings because of its extreme hardness, low friction coefficient, high melting point (2927 °C), golden color and low electrical resistivity (ca. 50 $\mu\Omega$ cm).[15] Typical applications are for cutting tools, in electronics (integrated circuits, diffusion barriers) and for decorative or protective coatings. The oxynitride films are equally interesting for such applications, while they offer an additional possibility of tuning of their properties by changing the O/N ratio.[12] TiN is a promising conductive additive for Li-battery materials, such as polyaniline[15] or Li-titanate spinel.[16] Applications of TiN as a catalyst have been reported, too.[17,18]

Because of the virtually identical X-ray diffraction patterns of TiO, TiO_xN_y, and TiN, as well as the problems associated with elemental analysis of these materials, the reports on direct nitridation of TiO_2 toward TiN[19−21] should be considered with care. The situation is further complicated by the existence of monoclinic TiO[8] and by three other crystal structures for substoichiometric titanium nitrides, viz. hexagonal α-TiN_x ($x < 0.33$), and two tetragonal phases Ti_2N,[22] but the hexagonal cell reported for TiN[23] is an obvious error. The nonstoichiometric TiN_x is selectively diagnosed by the Raman-active phonons from vacancies,[3,22,24] because the first-order Raman scattering is completely forbidden for the perfect TiN (osbornite)[3,22,24] as well as for the TiO_xN_y crystals.[11,12] A convenient method for distinction between TiN, TiO_xN_y, and TiO_2 (the usual impurity in samples) is the X-ray photoelectron spectroscopy (XPS) of the Ti core levels.[7−12]

TiN is usually prepared at temperatures of ca. 1200 °C from Ti-metal and N_2 or NH_3. An alternative high-temperature route is the so-called carbothermal reaction employing TiO_2 as a precursor[25]

$$TiO_2 + 2C + \frac{1}{2}N_2 \rightarrow TiN + 2CO \qquad (1)$$

Titanium nitride is also synthesized by a ligand-assisted ammonolysis from $TiCl_4bpy_n$ (bpy = 2,2′-bipyridine)[18] or from TiO_2 using molten cyanamide,[17] or sodium amide;[23] however, the products often contain carbon impurities (ca. 5%) because of incomplete removal of organic reactants. Synthesis of titanium oxynitride at 350 °C from $TiCl_4$ and NaN_3 was reported, too.[7]

There are several conflicting reports on the thermal nitridation of TiO_2 in NH_3 atmosphere, but to the best of our knowledge, there is no evidence of a complete conversion of TiO_2 into cubic oxynitride, TiO_xN_y occurring at temperatures ≤600 °C. Morawski et al.[5] did not find any other phase beyond anatase and rutile during the calcination of titania powder in the NH_3 atmosphere at temperatures up to 800 °C. On the other hand, Gao et al.[20] reported on a conversion of TiO_2 (anatase) powder into TiN in ammonia gas. The reaction occurred, reportedly, at 800 °C via Ti_2O_3 and TiO_2 (rutile) intermediates, but was incomplete at 700 °C.[20] Unfortunately, no detailed interpretation of the diffraction patterns was given and neither of the lattice constants were calculated in this paper.[20] Hence, the proof of TiN is insufficient, and we may speculate that TiO_xN_y could be mismatched with TiN. Mangamma et al.[19] reported on a conversion of TiO_2 to TiN taking place in the NH_3/Ar atmosphere at 1100 °C. Like in the previous case, the proof of TiN (against TiO_xN_y) does not seem to be evident. Gartner et al.[21] treated porous TiO_2 thin films in an NH_3 atmosphere at 600 °C. The product of this reaction was prevailingly amorphous with a weak XRD peak at around $2\Theta = 43°$ (CuKα), which was assigned to TiN or $TiN_{0.9}$ (osbornite).[21] Again, we may argue that cubic TiO_xN_y would give an analogous pattern.

The problem of direct nitridation of titanium oxides was further elucidated by Janik et al.[8] who studied the reaction of NH_3 with TiO_2 (anatase) and TiO (monoclinic). They have found that TiO converts to a phase-pure TiO_xN_y at 1000 °C, but the product made from anatase at 1000−1200 °C further contained TiO_2 rutile.[8] The mechanism of TiO_2/NH_3 reaction was studied in detail, highlighting the Lewis-acidic five-coordinated Ti^{4+} site on the surface, which acts as the reaction center for anchoring of NH_3 and for its subsequent chemical transformation toward $TiO_{2-x}N_x$[26] and eventually toward cubic nitride/oxynitride phases.[8,19−21]

Here we show, for the first time, that nanocrystalline electrospun titania (anatase) fibers are smoothly converted into cubic TiO_xN_y fibers by a heat treatment in ammonia atmosphere at temperatures ≤600 °C for 4 h. The precursor material is composed of nanocrystals ca. 10−30 nm in size, which are assembled in long fibers of typically 0.1−1 μm in diameter. Such materials are often called "nanofibers"[27,28] but terms like "nanocrystalline fibers" would be more accurate. The formed TiO_xN_y fibers are changeable back into the TiO_2 fibers (anatase or rutile) by calcination in air or oxygen. The TiO_2/TiO_xN_y conversion

(15) Qiu, Y.; Gao, L. *J. Phys. Chem. B* **2005**, *109*, 19732.
(16) Snyder, M. Q.; Trebukhova, S. A.; Ravdel, B.; Wheeler, M. C.; DiCarlo, J.; Tripp, C. P.; DeSisto, W. J. *J. Power Sources* **2007**, *165*, 379.
(17) Fischer, A.; Makowski, P.; Muller, J. O.; Antonietti, M.; Thomas, A.; Goettmann, F. *ChemSusChem* **2008**, *1*, 444.
(18) Kaskel, S.; Schlichte, K.; Kratzke, T. *J. Mol. Catal. A* **2004**, *208*, 291.
(19) Mangamma, G.; Ajikumar, A. P.; Nithya, R.; Sairam, T. N.; Mittal, V. K.; Kamruddin, M.; Dash, S.; Tyagi, K. *J. Phys. D: Appl. Phys.* **2007**, *40*, 4597.
(20) Li, J.; Gao, L.; Sun, J.; Zhang, Q.; Guo, J.; Yan, D. *J. Am. Ceram. Soc.* **2001**, *84*, 3045.
(21) Gartner, M.; Osiceanu, P.; Anastasescu, M.; Stoica, T.; Trapalis, C.; Giannakopoulou, T.; Todorova, N.; Lagoyannis, A. *Thin Solid Films* **2008**, *516*, 8184.
(22) Gyorgy, E.; Perez del Pino, A.; Serra, P.; Morenza, J. L. *Appl. Surf. Sci.* **2002**, *186*, 130.
(23) Huang, Y.; Gu, Y.; Zheng, M.; Xu, Z.; Zeng, W.; Liu, Y. *Mater. Lett.* **2009**, *61*, 1056.
(24) Bernard, M.; Deneuville, A.; Thomas, O.; Gargaud, P.; Sandstrom, P.; Birch, J. *Thin Solid Films* **2000**, *380*, 252.
(25) Ortega, A.; Roldan, M. A.; Real, C. *Int. J. Chem. Kinet.* **2005**, *37*, 566.
(26) Kuroda, Y.; Mori, T.; Yagi, K.; Makihata, N.; Kawahara, Y.; Nagao, M.; Kittaka, S. *Langmuir* **2005**, *21*, 8026.
(27) Frenot, A.; Chronakis, I. S. *Curr. Op. Colloid Interfac. Sci.* **2003**, *8*, 64.
(28) Jirsak, O.; Sanetrnik, O.; Lukas, D.; Kotek, V.; Martinova, L.; Chaloupek, J. WO 2005/024101 A1, 2005.

Scheme 1. Overview of the Studied Reactions[a]

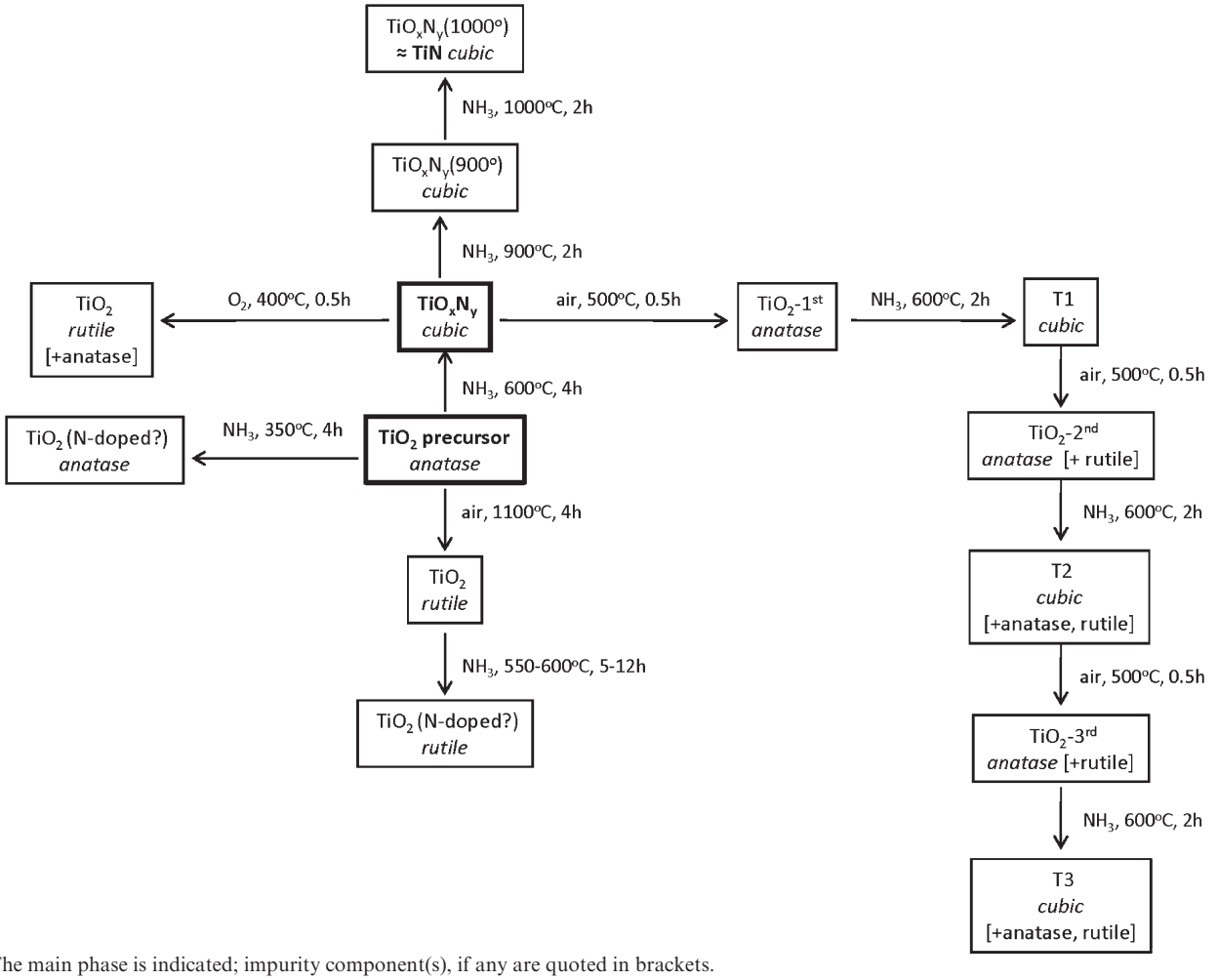

[a] The main phase is indicated; impurity component(s), if any are quoted in brackets.

occurring at ≤600 °C is specific for electrospun anatase fibers. Other forms of nanocrystalline anatase do not react with ammonia creating TiO_xN_y under these gentle conditions. Further, we show that phase-pure TiN fibers can be grown from TiO_xN_y fibers in ammonia at temperatures up to 1000 °C.

2. Experimental Section

2.1. Preparation of Nanocrystalline TiO_2 Fibers. The precursor for electrospinning was prepared as follows. Titanium butoxide (100 g) was dissolved in 250 g of ethanol and 29.4 g of acetylacetone was added. The resulting solution was carefully mixed with a solution of 35.2 g poly(vinylpyrrolidone), MW = 1 300 000 in 758.8 g ethanol. Finally small amount of HCl was added dropwise. This solution was used for the preparation of nanocrystalline fibers by means of electrospinning[27] using the industrial Nanospider technology.[28] In this manufacturing process, fibers are grown from the surface of a rotating cylinder covered with the polymer solution thin layer, instead of the conventional nozzle tip. To burn out the organic components from fibers, we calcined the product at 500 °C in an air atmosphere. Thus prepared titanium dioxide fibers were in the form of felt. They contained phase pure anatase and had surface areas of 40−60 m^2/g (depending on the batch) determined from the nitrogen adsorption isotherms (see below). Rutile fibers were prepared by the calcination of anatase fibers at 1100 °C in air.

2.2. Reaction of TiO_2 with NH_3. The reaction was carried out in a vertical quartz-tube furnace, which was purged with NH_3 (Messer, purity 3.8) upwardly. The ammonia outlet pipe was on the top of the quartz tube, and the exhaust gas was fed through a bubbler filled with water. The sample of fibrous TiO_2 material was positioned inside the fluid bed quartz tube reactor and fixed in the hot zone using quartz-fiber padding which served as a sample holder. The flow of ammonia was regulated by a gas-dosing valve and was about 40−60 mL/min. The temperature and heating ramp was controlled by a programmer (Detlef Gestigkeit, PR5 3 T) equipped with a K-type thermocouple. Scheme 1 is the survey of main reactions that were carried out with our fibrous TiO_2 (anatase) precursor at various conditions.

2.3. Methods. The BET (Brunauer, Emmett, Teller) surface areas of the prepared materials were determined from nitrogen adsorption isotherms at 77 K using the Micromeritics ASAP 2020 instrument. Before the adsorption measurement, all samples were degassed at 300 °C overnight. Scanning electron microscopy and energy-dispersive X-ray analysis (EDX) were carried out using the Hitachi FE SEM S-4800 microscope equipped with the Noran EDX system. Powder X-ray diffraction (XRD) was studied on a Bruker D8 Advance diffractometer using CuKα radiation and the lattice constant was evaluated using the ZDS software package.[29] The exact positions of diffraction peaks (in 2 Θ) were evaluated by profile fitting analysis and indexed after

(29) Ondrus,P. *ZDS software for X-ray powder diffraction pattern analysis, version 5.14*; ZDS System: Praha, Czech Republic, 1995.

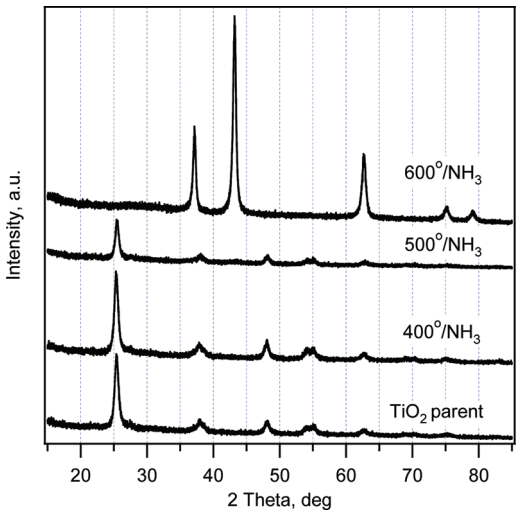

Figure 1. X-ray diffraction patterns of the parent TiO_2 (anatase) fiber sample and the products of its reaction with NH_3 at various temperatures. The curves are offset for clarity, but the intensity scales are identical for all samples.

comparison with values calculated from lattice constant of pure TiN. Subsequently, the lattice constant of TiO_xN_y was refined. The XPS measurements were carried out using VG ESCA3MkII spectrometer equipped with an Al Kα X-ray source and electrostatic hemispherical electron analyzer. The spectrometer was operated in the fixed analyzer transmission mode. The pressure of residual gases in analyzer chamber during spectra accumulation was 3×10^{-8} mbar. The estimated error in binding energy determination was ±0.1 eV. Theoretical photoionization cross sections were used to convert peak integrated intensities into the elemental concentrations.[30] Curve fitting of overlapping spectral lines was carried out using the lines of a Gaussian−Lorentzian shape and the damped nonlinear least-squares technique. XPS measurement was also interfaced to gentle Ar^+ sputtering (5 keV, 20 μA, 5 min). Systematic analysis of XPS sputter-depth profiles was not possible, because our samples were sensitive to chemical degradation of the surface upon prolonged sputtering (see the Supporting Information, S1).

3. Results and Discussion

3.1. Conversion of TiO_2 into TiO_xN_y Fibers. Figure 1 shows X-ray diffraction patterns of the parent TiO_2 (anatase) fiber sample and those of the products of the TiO_2/NH_3 reaction at various temperatures between 400 and 600 °C (from bottom to top). The heating ramp was 32 °C/min and the time of reaction at the final temperature (in °C; see annotation in Figure 1) was 4 h. The sample was cooled in the NH_3 flow for 2 h after completion of the reaction. It is obvious that the fibers keep the parent crystal structure of anatase up to 500 °C. Afterward, there is a sudden conversion of anatase fibers into a material having the X-ray diffraction pattern of cubic rock-salt structure between 500 and 600 °C. More precisely, the reaction starts at around 550 °C, when both TiO_2 (anatase) and cubic phase have been traced in various proportions depending on the batch. The white TiO_2 fibers turn their color to yellow at ca. 300−350 °C and to yellow-green at ca. 400 °C. These low-temperature intermediates are very probably N-doped TiO_2 (anatase) fibers. They are of interest for application in photocatalysis, but the investigation of N-doped TiO_2 is beyond the scope of this paper.

The reaction product formed at 600 °C was a phase-pure cubic material (Figure 1 top curve). Its lattice constant was: $a = 4.1930(6)$ Å, which points at the TiO_xN_y. Some authors calculated the stoichiometric coefficients x, y from the Vegard's law[7]

$$a_{TiON} = xa_{TiO} + ya_{TiN} \quad (2)$$

(a_{TiON}, a_{TiO}, and a_{TiN} are the lattice constants of TiO_xN_y, TiO, and TiN). However, other authors pointed out that the application of Vegard's law is questionable for nanocrystals and defect structures.[8] In our case, the coefficients, calculated from eq 2 and $a = 4.1930(6)$ Å, would give the composition of about $TiO_{0.7}N_{0.3}$ (assuming $x + y = 1$, that is oxygen substitutes N in the TiN structure[9]). EDX analysis gave 40 at % Ti, 38 at % O, and 21 at % N (calcd for $TiO_{0.7}N_{0.3}$: 50 at % Ti, 35 at % O and 15 at % N). Admitting large experimental errors (±5 at %) of EDX analysis of the Ti−O−N system, the expected sample composition is roughly supported, but we cannot rule out the presence of some impurities, such as "amorphous" TiO_2 (see the next paragraph). Other physical properties of our TiO_xN_y are listed in Table 1. The crystallite size, d_c (coherent length of the crystal domain), was calculated from X-ray line broadening (w) according to the Scherrer formula

$$d_c = 0.9\lambda/w\cos\Theta \quad (3)$$

where λ is the X-ray wavelength, 0.1540562 nm (CuKα), and Θ is the diffraction angle.

The XPS analysis of this sample gave the surface stoichiometry of O/Ti = 1.54 to 1.75 and N/Ti = 0.64 to 0.77 (for various sample batches). Obviously, the surface concentrations of nitrogen and oxygen are larger than those for the predicted stoichiometry ($TiO_{0.7}N_{0.3}$) but the experimental O/N ratios are surprisingly well matching the expected value of 2.3. There were no other impurities beyond the usual adventitious carbon contaminant and trace amount of potassium (K/Ti = 0.04) whose origin is unknown.

The Ti $2p_{3/2}$ line is known to be at the binding energies of (454.7−455.1) eV; (456.0−456.7) eV and (458.1−458.3) eV for TiN, TiO_xN_y, and TiO_2, respectively.[7−12] On the other hand, the N 1s line is around (396.0−396.9) eV for both TiN and TiO_xN_y. In our case, Figure 2 (left panel) shows the N 1s line with a major peak at 396.5 eV, and the minority lines located at 398.3 and 400.3 eV, which could be assigned to characteristic energy losses[31] or might be due to adsorbed NH_x species. The Ti $2p_{3/2}$ photoemission line (Figure 2 middle panel) can be fitted into two components at 456.2 eV (ca. 35%) and 458.5 eV (ca. 65%). The latter line indicates the presence of TiO_2,

(30) Scofield, J. H. *J. Electron Spectrosc. Relat. Phenom.* **1976**, *8*, 129.

(31) Strydom, I. R.; Hofmann, S. *J. Electron Spectrosc. Relat. Phenom.* **1991**, *56*, 85.

Table 1. Properties of the Studied Materials[a]

sample	phase	composition	surface area, S_{BET} (m^2/g)	crystallite size, d_c (nm)	lattice const., a (Å)
TiO_2 precursor	anatase	(TiO_2)[b]	43−53[c]		
TiO_xN_y	cubic	$TiO_{0.95}N_{0.53}$	43.6	16	4.1930 ± 0.0006
T1	cubic	$(TiO_xN_y + TiO?)$[b]	49.1	14	4.171 ± 0.002
T2	cubic	$(TiO_xN_y + TiO?)$[b]	59.0	11	4.173 ± 0.002
T3	cubic	$(TiO_xN_y + TiO?)$[b]	71.7	10	4.174 ± 0.001
TiO_xN_y (900°)	cubic	$TiO_{0.11}N_{0.85}$	15.1	14	4.2093 ± 0.0007
TiO_xN_y (1000°)	cubic	$TiO_{0.004}N_{0.96}$	4.8	30	4.2290 ± 0.0001

[a] Composition of products is based on EDX analysis unless stated otherwise. Titanium oxynitride, TiO_xN_y, fibers are grown by ammonia nitridation at 600 °C from the TiO_2 precursor (S_{BET} = 43.6 m^2/g). The phases T1−T3 are products of subsequent conversion cycles of air oxidation/ammonia nitridation of TiO_xN_y. [b] Assumed composition based on XRD, XPS, and EDX; anatase and rutile impurities detected in T2 and T3 (see text for details). [c] Depending on the sample batch.

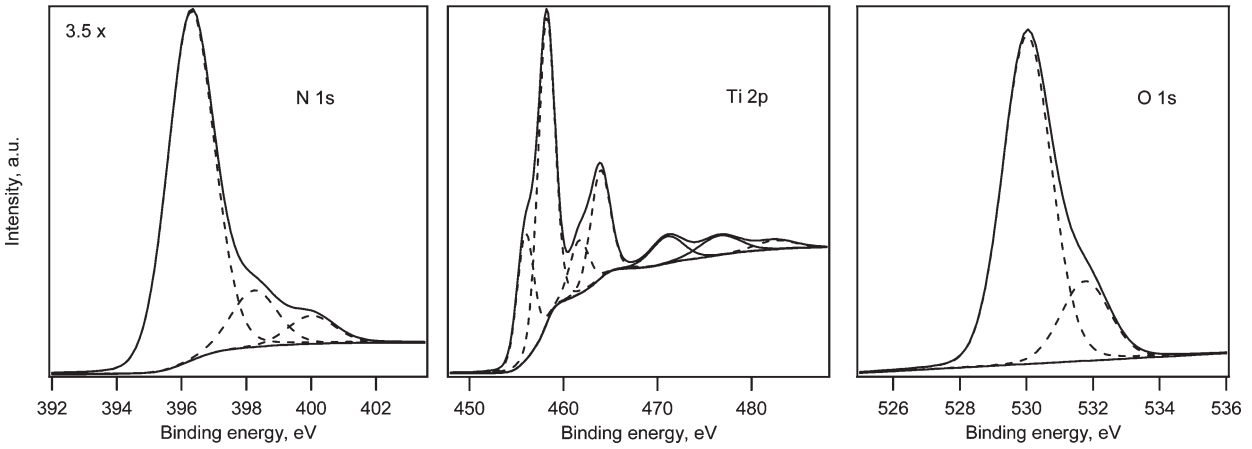

Figure 2. X-ray photoelectron spectra for the TiO_xN_y fibers in the region of binding energies of N 1s, Ti 2p, and O 1s core levels. The intensity scale is comparable in all panels, and is zoomed by a factor of 3.5 in the left chart.

and the former one is diagnostic for oxynitride, TiO_xN_y.[8−12] This assignment is consistent with the spectra of O 1s photoelectrons (Figure 2 right panel), composed of two components centered at 530.2 and 531.8 eV, characteristic of Ti oxide and Ti oxynitride, respectively.[4] The detection of TiO_2 by XPS is somewhat surprising, because TiO_2 was not found by XRD (Figure 1). We may speculate that this TiO_2 is "amorphous", but a similar problem was mentioned also by other authors[8,11] who have concluded that TiO_2 is formed solely on the surface of titanium nitride/oxynitride during air exposure before the XPS measurement. Hence, XPS could not prove unequivocally the presence of unreacted TiO_2 in the samples.[8,11]

Figure 3 presents scanning electron micrographs (SEM) of the parent TiO_2 (anatase) fibers (Figure 3A,B) and the corresponding TiO_xN_y fibers (Figure 3C,D). It is obvious that the fibrous structure of the TiO_2 precursor is preserved also in the TiO_xN_y product, and the primary particles of the latter are coarser. This illustrates also the found 15−55% drop of S_{BET} (growth of particles size) during the TiO_2/TiO_xN_y conversion as discussed above. In the absence of ammonia, the morphology of our TiO_2 (anatase) precursor is slightly changed as a result of heat treatment at 600 °C (cf. Figure 3A against Figure 3B). The nanostructure of calcined fibers (Figure 3B) becomes rougher and more open, which may enhance the reactivity toward NH_3.

The conversion of TiO_2 fibers into TiO_xN_y manifested itself by a marked color change from white to black. The annealing of TiO_2 fibers at 600 °C in NH_3 atmosphere caused a 15−55% drop of the BET surface area. The specific surface area decrease of the particular samples was dependent on their original morphology. It was more pronounced for TiO_2 fibers with a smaller BET surface area and vice versa. For instance, a reaction of TiO_2 fibers with S_{BET} of 52.6 m^2/g with ammonia provided the TiO_xN_y product with S_{BET} of 43.6 m^2/g, whereas the same treatment of fibrous TiO_2 exhibiting S_{BET} of 43 m^2/g led to a TiO_xN_y product with the surface area of only 20 m^2/g.

3.2. Nitridation of Other TiO_2 Materials. To check whether or not other forms of nanocrystalline titania convert analogously to TiO_xN_y at the same conditions, we have selected two commercial TiO_2 powders for comparative tests: Bayer PKP0904, (S_{BET} = 154 m^2/g, pure anatase, d_c = 10 nm), and Degussa P-25 (S_{BET} = 47.5 m^2/g, anatase/rutile mixture; 70/30%, d_c = 30 nm).[32] These powders were exposed to ammonia flow at temperatures from 500 to 600 °C. In all cases, the reaction products were pale yellow N-doped titania, $TiO_{2-x}N_x$ (x ranged from 0.02 to 0.05). They exhibited the tetragonal XRD patterns of anatase (sometimes with small amount of rutile) but the formation of cubic nitride/oxynitride phase was not observed. According to the XPS analysis, about 25−40 at% of nitrogen had the N

(32) Kavan, L.; Grätzel, M.; Rathousky, J.; Zukal, A. *J. Electrochem. Soc.* **1996**, *143*, 394.

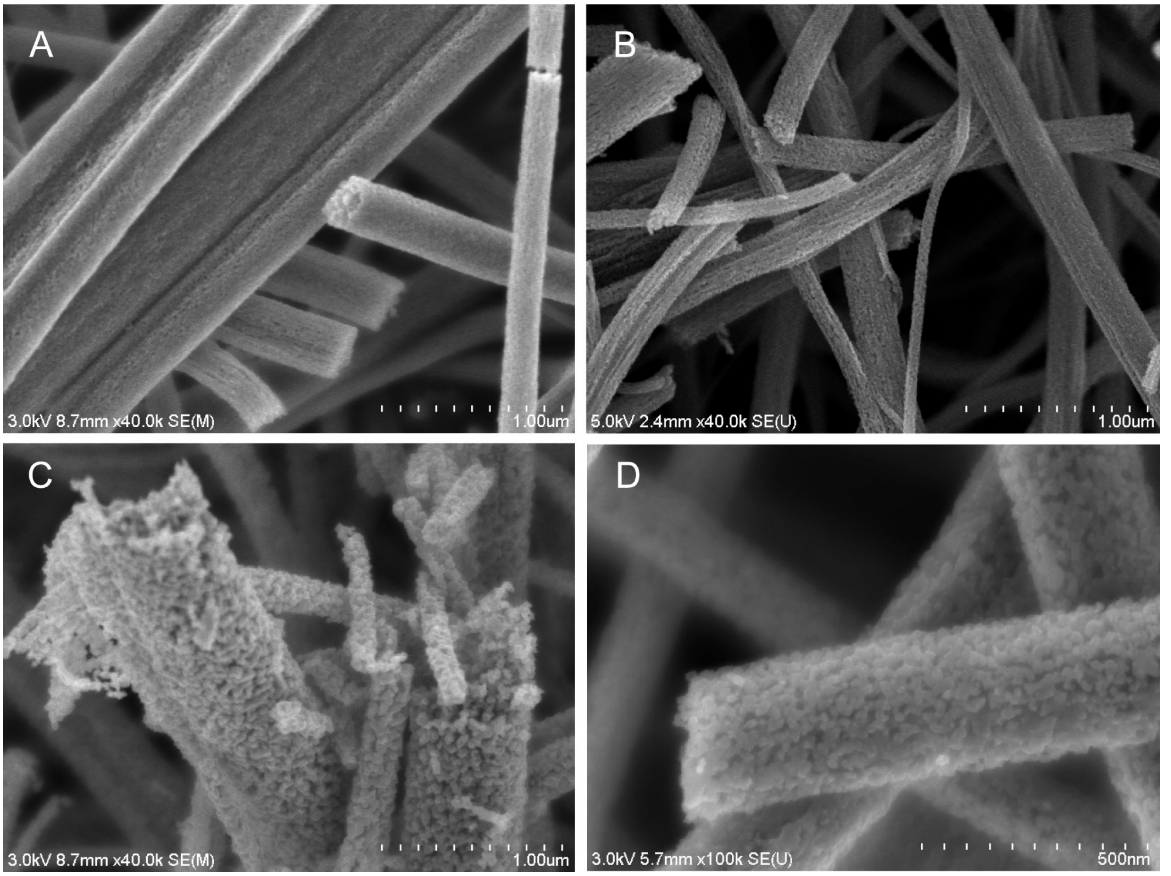

Figure 3. Scanning electron microscopy images of (A) the parent TiO_2 (anatase) made by electrospinning, (B) the same sample calcined at 600 °C/4 h, and (C, D) TiO_xN_y fibrous product grown in ammonia at 600 °C/4 h. Picture size: (A−C) $3 \times 2.3\ \mu m^2$ and (D) $1.3 \times 0.9\ \mu m^2$.

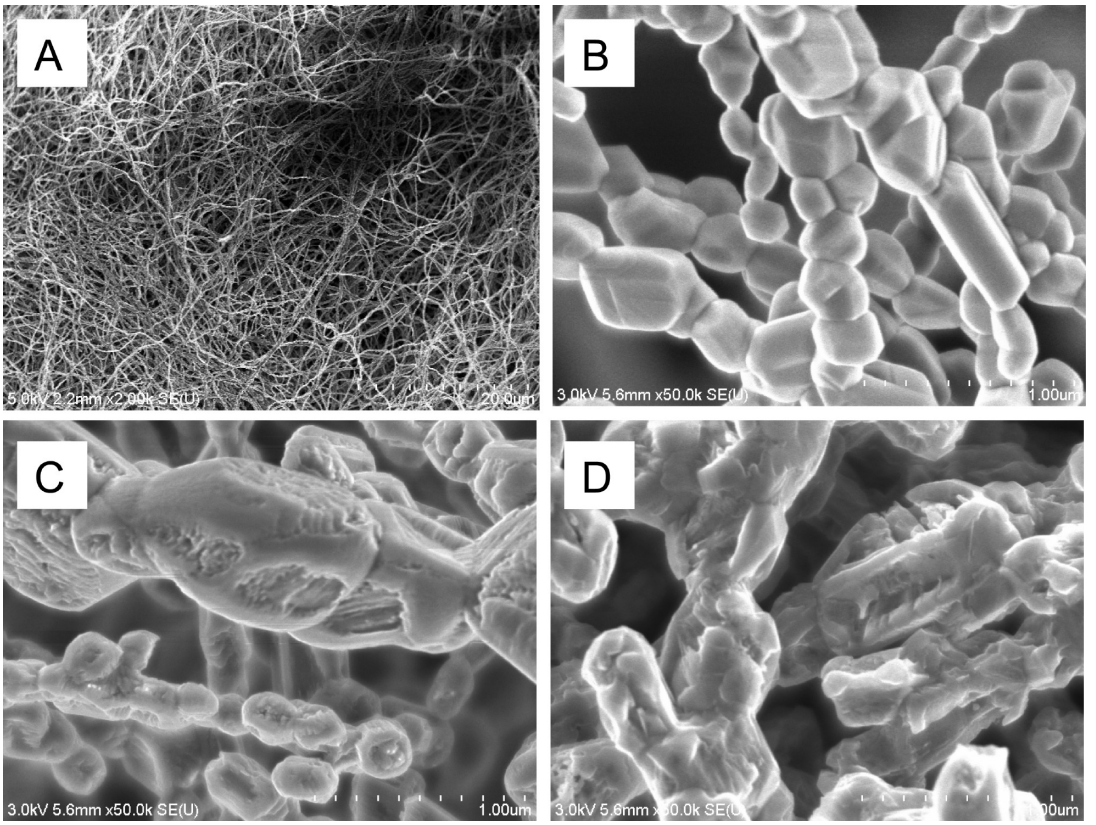

Figure 4. Scanning electron microscopy images of (A, B) TiO_2(rutile) fibers grown from TiO_2(anatase) at 1100 °C. The products of their reaction in NH_3 stream at (C) 600 °C/5 h and (D) 600 °C/12 h are also shown. Image size: (A) $58 \times 44\ \mu m^2$ and (B−D) $2.5 \times 1.9\ \mu m^2$.

1s binding energy of 396.2 ± 0.2 eV, which in this case, indicates the lattice nitrogen doping; the rest was adsorbed ammonia with the N 1s binding energy of 400.1 ± 0.2 eV (data not shown). This matches the conclusion of others[1,2,5] that the TiO_2/NH_3 reaction (occurring at 600 °C) stops at the stage of N-doped titania, and no TiO_xN_y nor TiN is formed. Our comparative tests confirm that the electrospun TiO_2 fibers are exceptionally reactive toward nitridation producing cubic oxynitrides, TiO_xN_y in ammonia flow at 600 °C. Powder titania materials do not seem to show this reactivity, independent of the phase composition (anatase/rutile, BET area and particle size).

The fact that the nitridation of TiO_2 toward TiO_xN_y depends significantly on the morphology and/or crystal phase was supported by another reference experiment. It used TiO_2 (rutile) fibers, which were grown from our raw anatase fibers at 1100 °C (see Experimental Section and Scheme 1). Figure 4A confirms the overall shape retention of fibrous morphology even at this temperature, even though the fibers are composed of large rutile crystals typically of 100−200 nm in size (Figure 4B). These fibers were calcined in NH_3 stream at 550 °C/5 h, 600 °C/5 h and 600 °C/12 h. Although the samples turned black, no cubic TiO_xN_y was detected by XRD (data not shown). There is an obvious change in the crystal facets appearance: The pristine rutile crystals, are attacked by NH_3 on the edges, and gradually convert to materials with massive surface erosion (Figure 4 C,D). The question whether or not fibrous rutile of the same morphology, particle size and porosity like our raw anatase fibers (Figure 3A) would react toward TiO_xN_y cannot be addressed at this stage of research, because such reference rutile fibers (with particle sizes of ca. 10−20 nm) are not available. We may only suggest that there is an indirect argument supporting that nanocrystalline fibrous rutile would probably react similarly (see section 3.3 for further discussion).

3.3. Oxidation of TiO_xN_y Fibers. The TiO_xN_y sample grown from anatase TiO_2 fibers at 600 °C in NH_3 (as in Figure 1) was subjected to heat treatment in air or oxygen at various temperatures (see Scheme 1). Figure 5 shows X-ray diffraction patterns of typical products. The heating ramp was 40 °C/min and the reaction time was 30 min (the reaction temperatures (in °C) are indicated by annotations in Figure 5). The described reaction is similar to that reported by Cui et al.[6] who annealed the TiN powder (40 nm particle size) in air at 350 °C. It is obvious that our TiO_xN_y fibers convert spontaneously to TiO_2 (anatase) at 450 °C in air. When the reaction temperature increases, a small portion of rutile is also formed as the second phase. The rutile phase (diffraction peak at $2\Theta \sim 27$ deg, Figure 5) starts to be detectable at 550 °C/air (Figure 5) and its content slightly increases with the calcination temperature in air. It is interesting to note that, in TiO_2, the transition temperature of anatase-rutile conversion is quite close, between 500 and 550 °C.[33] Nevertheless this similarity seems to be a casual coincidence only, because

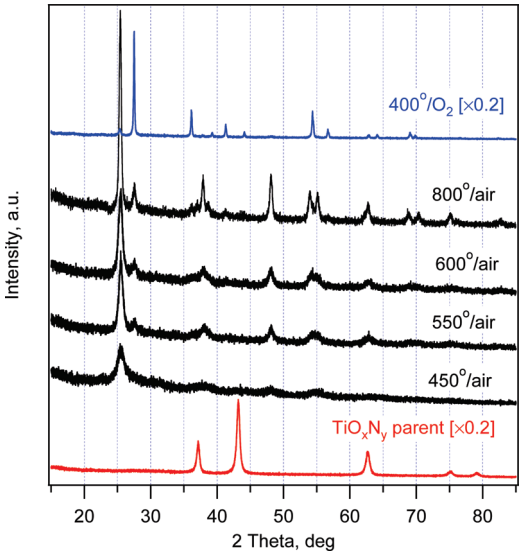

Figure 5. X-ray diffraction patterns of the TiO_xN_y fiber sample (bottom curve) and the products of its heat treatment in air or oxygen at various temperatures (see labels on each curve). The diffractograms of the starting TiO_xN_y (bottom curve) and the product of calcination in oxygen (top curve) are scaled by a factor of 0.2 in the diffraction intensity. The curves are offset for clarity.

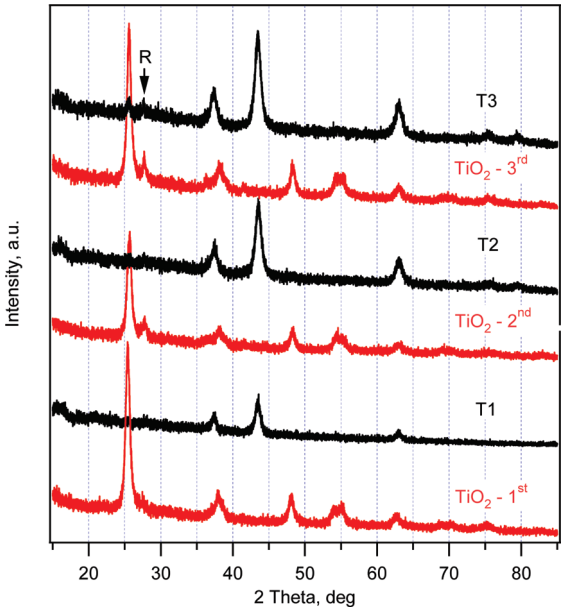

Figure 6. X-ray diffraction patterns of a TiO_2 (anatase) fiber (bottom red curve), which was converted at 600 °C in NH_3 and back to TiO_2 (anatase/rutile) in air at 500 °C. Three subsequent cycles of these conversions are documented by curves from bottom to top. The curves are offset for clarity, but the intensity scales are identical for all samples. The main peak of rutile is labeled by R.

the formation of TiO_2 (rutile) from TiO_xN_y is more significantly accelerated by an increase of oxygen concentration in the surrounding atmosphere rather than by the temperature. For instance, in pure oxygen at 400 °C, the TiO_xN_y turned its color from black to white within seconds. Figure 5 (top curve) shows that this sample is composed from TiO_2 rutile and small amount of anatase. Scanning electron micrograph (see the Supporting Information, Figure S2) shows that the product is a fused compact material with small amount of residual fibers.

(33) Depero, L. E.; Bonzi, P.; Zocchi, M.; Casale, C.; De Michele, G. *J. Mater. Res.* **1993**, *8*, 2709.

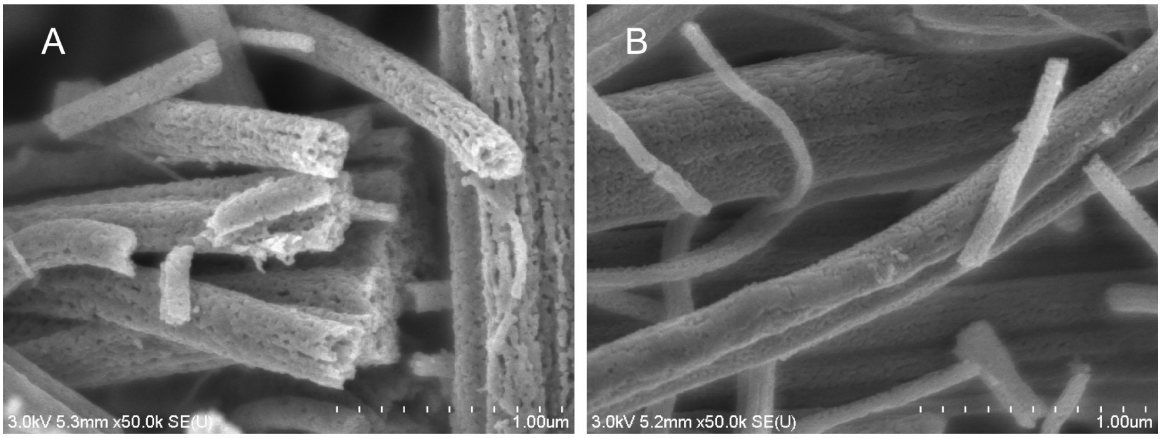

Figure 7. Scanning electron microscopy image of (A) TiO_2-2nd generation and (B) the last nitridation product T3. Picture size 2.5 × 1.9 μm^2 in both cases.

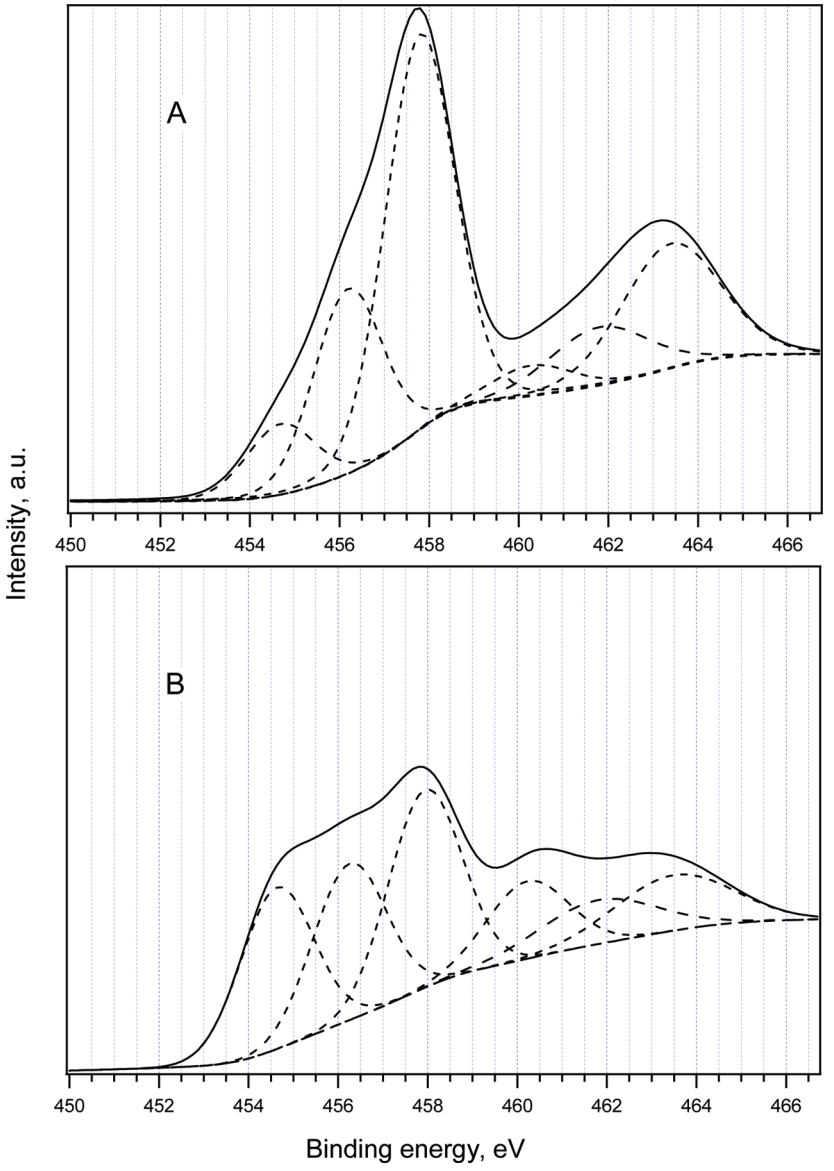

Figure 8. X-ray photoelectron spectra for the T2 fibers in the region of binding energies of Ti 2p core levels. (A) Sample "as-received", (B) sample after Ar^+ sputtering.

In contrast, if the TiO_xN_y calcination is carried out in the air, even at 800 °C, the fibrous morphology of the starting oxynitride material (cf. Figure 3B) is still preserved and only traces of rutile are detected (Figure 5).

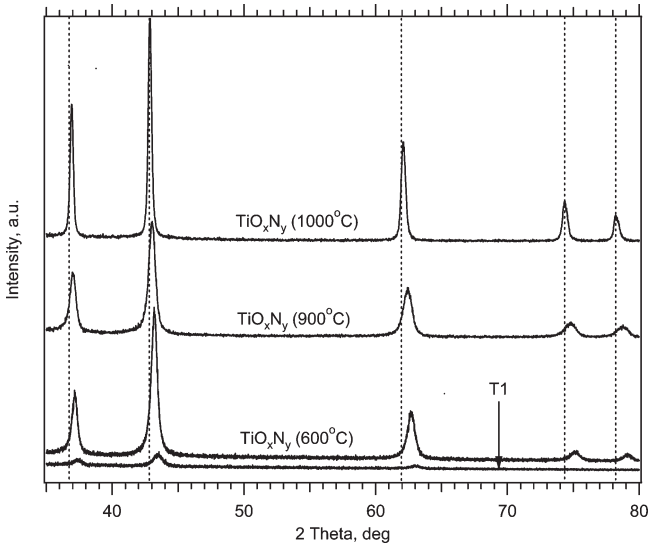

Figure 9. X-ray diffraction patterns of the samples produced by the reaction of titania fibers with NH_3 at various temperatures. The curves are offset for clarity, but the intensity scales are identical for all samples. Dashed lines indicate the expected positions of diffraction peaks of TiN.

The TiO_xN_y sample grown from anatase TiO_2 fibers at 600 °C in NH_3 (as in Figure 1) was subjected to several other oxidation/nitridation reactions (see Scheme 1). The TiO_xN_y was oxidized at 500 °C in air for 30 min producing almost pure TiO_2 (anatase) labeled TiO_2-1st (Figure 6). The temperature of 500 °C was chosen as optimum for growth of reasonably crystalline anatase which was almost free from rutile (cf. also Figure 5, traces 450°/air and 550°/air). This material was further exposed to NH_3 at 600° for 2 h, and the reaction transformed it again into a pure cubic phase labeled T1 (Figure 6). This procedure was repeated two times, whereas the next two generations of cubic phases were grown, T2 and T3 with the corresponding intermediates TiO_2-2nd and TiO_2-3rd (Figure 6). The cyclic conversion was reasonably reversible, although there was a growing proportion of rutile in each next generation of TiO_2-*n*th. The rutile impurity in TiO_2-2nd was consumed to a great extent during the formation of T2, and this effect was reproduced also for the TiO_2-3rd/T3 conversion (cf. Figure 6). We therefore suggest that trace rutile, which is presumably also fibrous and nanocrystalline, is reactive toward nitridation as the fibrous anatase is.

The basic properties of T1−T3 are summarized in Table 1: it is obvious that each next generation of the products shows smaller crystallite sizes (larger S_{BET}) and this trend is monotonous even if we include the parent TiO_xN_y as the "zero generation" material. The disintegration of originally coarse particles of TiO_xN_y (Figure 3B) during the described cyclic conversion is also documented by SEM (Figure 7).

The higher-generations cubic phases (T2, T3) also contain trace anatase impurities, revealed by diffraction peak at $2\Theta \approx 25°$ (Figure 6). The peak of anatase is quite narrow in the T3 material (Figure 6, top curve) indicating coarse sintered anatase particles, which are not convertible into cubic phase in NH_3 atmosphere. This mimics the behavior of ordinary nanocrystalline anatase, which was studied by others[1,2,5] and by ourselves for reference (vide ultra).

The found lattice constants of T1−T3 (Table 1) seem to point at cubic TiO (a = 4.173 Å).[8] However, the situation is more complex. Figure 8 shows the Ti 2p X-ray photoelectron spectrum of sample T2 as-received and also after gentle Ar^+ sputtering (5 keV, 20 μA, 5 min). The results for samples T1 and T3 (data not shown) were similar. The surface analysis of T2 gave N/Ti = 0.68, O/Ti = 1.96 (before sputtering) and N/Ti = 0.59, O/Ti = 1.76 (after sputtering).

The binding energies of $Ti2p_{3/2}$ photoelectrons (relative populations in parentheses) were found to be 454.7 eV (34%), 456.3 eV (27%), and 458.0 eV (39%). The latter component is obviously assignable to TiO_2 which was detected even by XRD in this particular case (see above), and the middle line (456.3 eV) stands for TiO_xN_y. The interpretation of the lowest-energy line (454.7 eV) is less clear. Its position seems to be diagnostic for TiN, but titanium monoxide, TiO, would have its $Ti2p_{3/2}$ photoemission line at a very similar binding energy, too.[34] Indeed, TiO is expected to be the main crystalline component in T1−T3 based on the cubic lattice constant (see Table 1 and discussion above), but T1−T3 obviously contain some proportion of oxynitrides, too. Moreover, this example demonstrates that the distinction of TiO and TiN is not straightforward by XPS, which is quite often neglected in the relevant literature about titanium nitrides/oxynitrides.

3.4. Conversion of TiO_xN_y into TiN Fibers. Finally, we have explored whether or not fibrous TiN is accessible via our reaction. To that purpose, we treated the TiO_xN_y (grown at 600 °C; cf. data in Figures.1-3,5 and Table 1) again in NH_3 stream at 900 °C for 2 h, cooled to room temperature, and subsequently recalcined in NH_3 stream for next 2 h at 1000 °C (see Scheme 1). Figure 9 shows the XRD curves of thus obtained samples, viz. TiO_xN_y(900°) and TiO_xN_y(1000°), respectively. The calculated lattice constants were: 4.2093(7) Å and 4.2290(1) Å, respectively. For comparison, Figure 9 shows the diffractograms of the starting material TiO_xN_y (600 °C) (as in Figure 1) and also T1 (as in Figure 6; its lattice constant is that of TiO). Vertical dashed lines in Figure 9 mark the positions of diffraction lines of pure TiN. They were obtained by measurement of a reference sample TiN (Aldrich; a = 4.2376(7) Å) at the same conditions, and they are practically identical to the database values (JCPDS #38−1420). We may conclude that our sample TiO_xN_y(1000°) is close to the stoichiometric TiN (that is $x \approx 0$, $y \approx 1$). This finding was supported by EDX analysis, that gave 51.1 at % N, 48.7 at% Ti, and 0.2 at% O.

Figure 10 shows the spectrum of Ti $2p_{3/2}$ photoelectrons of TiO_xN_y(1000°) as received and that after gentle Ar^+ sputtering (5 keV, 20 μA, 5 min). The surface analysis gave N/Ti = 1.05, O/Ti = 1.70 (before sputtering) and

(34) Bartkowski, S.; Neumann, M.; Kurmaev, E. Z.; Fedorenko, V. V.; Shamin, S. N.; Chekashenko, V. M.; Nemmonov, S. N.; Winiarski, A.; Rubie, D. C. *Phys. Rev. B* **1997**, *56*, 10656.

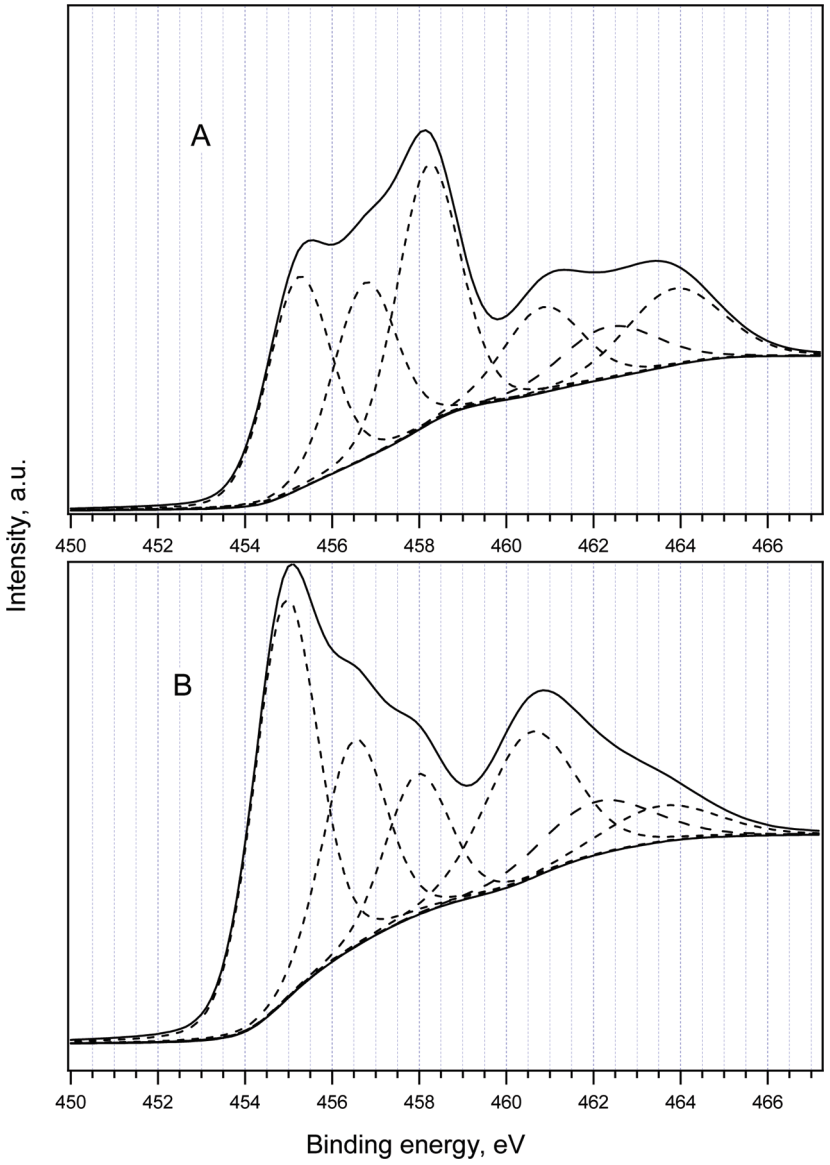

Figure 10. X-ray photoelectron spectra for the TiO_xN_y (1000 °C) sample in the region of binding energies of Ti 2p core levels. (A) Sample "as received", (B) sample after Ar^+ sputtering.

N/Ti = 0.98, O/Ti = 0.79 (after sputtering). This confirms the conclusion from EDX that this sample is nearly stoichiometric TiN, albeit XPS demonstrates also a massive surface oxidation. The binding energies of $Ti2p_{3/2}$ (relative population and assignment) were found to be: 455.2 eV−34%−TiN; 456.8 eV−27%−TiO_xN_y and 458.3 eV−39%−TiO_2. It is obvious that the oxygen-containing species are surface impurities, which are negligible in terms of bulk composition of this sample. This matches the conclusion of others,[8,11] corroborating the fact that the spectrum as in Figure 10 might, indeed, be assignable to a nearly perfect TiN.

SEM images shown in Figure 11 demonstrate that our two high-temperature samples still maintain the morphology of fibers composed from quite small particles. This is confirmed by XRD line broadening (Scherrer formula, eq 3 and data in Figure 9) which gives the d_c values of 14 and 30 nm for the phases grown at 900 and 1000 °C, respectively. The fact that the d_c values are similar or even smaller than those of the TiO_xN_y precursor (Table 1) is interesting in view of the massive crystal growth observed during heat treatment of TiO_2 fibers in air (cf. Figure 4A). However, these small particles are fused by sintering into quite compact fibers (Figure 11) exhibiting relatively small BET surface areas (Table 1). The synthesis of pure TiN fibers is another unique reaction of our electrospun titania materials.

We have no simple explanation for the distinctive reactivity of our anatase fibers grown by electrospinning. Surface analysis by XPS did not reveal any significant impurities on the surface of the parent anatase fibers, except for the usual C 1s signal of adventitious carbon and trace amount of potassium, the occurrence of which is unclear. Nevertheless, we can hardly speculate about some specific catalytic process, which would accelerate the TiO_2/TiO_xN_y/TiN conversion in our fibers. Two other methods of phase analysis were used to characterize our anatase fibers: Raman spectroscopy and Li-insertion electrochemistry (data

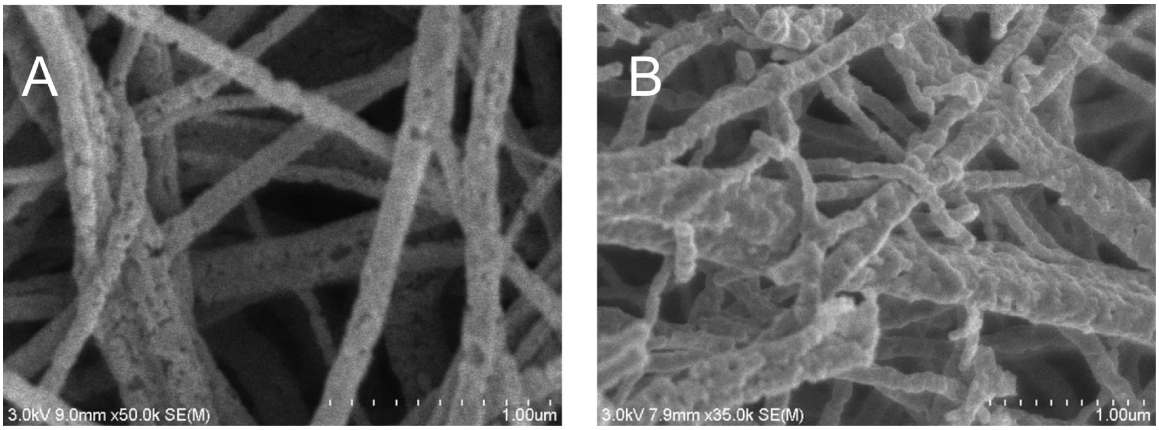

Figure 11. Scanning electron microscopy images of (A) TiO_xN_y (900 °C), image size, 2.5 × 1.9 μm^2; and (B) TiO_xN_y (1000 °C), image size, size 3.5 × 2.6 μm^2.

not shown here). Particularly, the electrochemical tests are known to be very sensitive to trace amounts of phase impurities in titania.[35,36] However, neither electrochemistry nor Raman revealed any other phases beyond anatase. This leads to a conclusion that the specific fiber properties, such as favorable surface area and accessibility, coupled with small anatase nanocrystals are responsible for their unique reactivity toward NH_3. We suggest that the perfectly open surface with limited number of sintered aggregates is beneficial for the solid/gas reaction. This conclusion is of a general impact. It would qualify our electrospun nanocrystalline fibers as promising materials for other applications, in which the heterogeneous reactions play a role, such as in catalysis and photocatalysis. The facile method of producing electrically conducting and ultrahard nanocrystalline fibers is of a clear application potential, too.

4. Conclusions

New low-temperature synthesis of nanocrystalline cubic TiO_xN_y with fibrous morphology was found. The fibers of TiO_2 (anatase) made by Nanospider technology can be converted into TiO_xN_y fibers by a reaction with NH_3 and back to TiO_2 (anatase) by air oxidation. The TiO_2/TiO_xN_y transformation occurs at temperatures as low as ca. 550 °C, whereas the TiO_xN_y oxidation occurs even lower, at 450 °C. The process is essentially reversible, although there is a small retention of unconvertible TiO_2 (anatase) and TiO_2 (rutile) in higher generations of products.

In pure oxygen, the fibrous TiO_xN_y transforms into fused rutile crystals at 400 °C, while in the air, anatase fibers are produced as the main phase even at temperatures as high as 800 °C.

Because of very similar XRD patterns, the identification of various phases in the system (TiN, TiO_xN_y, TiO) requires accurate calculation of lattice constant, as well as supporting experiments, such as X-ray photoelectron spectroscopy of the Ti2p core levels and elemental analysis.

Ordinary titania powders do not react toward TiO_xN_y at the same conditions independent of their phase composition (anatase/rutile), particle size and S_{BET}. The same conclusion applies for coarse fibrous rutile grown from our raw anatase fibers at 1100 °C. No cubic phase was detected by XRD even after 12 h in NH_3 flow at 600 °C. This work points to the general importance of the fibrous morphology of nanocrystals and accessibility of the surface for heterogeneous solid state reactions.

The synthesis of nearly perfect TiN was demonstrated via subsequent nitridation of TiO_xN_y (grown at 600 °C) in ammonia stream at temperatures up to 1000 °C. This material still keeps the morphology of fibers that are composed from sintered nanocrystals. The crystal size of TiN is not much different from that of the precursor.

Acknowledgment. This work was supported by the Czech Ministry of Education, Youth and Sports (Contracts LC-510, MSM002160857 and COST D35 OC09048) and by the Academy of Sciences of the Czech Republic (Contracts IAA 400400804 and KAN200100801).

Supporting Information Available: Photoelectron spectra (XPS) of a reference TiO_2 anatase precursor and that after Ar^+ sputtering (Figure S1); scanning electron microscopy image of a material prepared by heat treatment of TiO_xN_y fibers in pure oxygen at 400 °C (Figure S2) (PDF). This material is available free of charge via the Internet at http://pubs/acs/org/.

(35) Zukalova, M.; Kalbac, M.; Kavan, L.; Exnar, I.; Grätzel, M. *Chem. Mater.* **2005**, *17*, 1248.
(36) Prochazka, J.; Kavan, L.; Shklover, V.; Zukalova, M.; Frank, O.; Kalbac, M.; Zukal, A.; Pelouchova, H.; Janda, P.; Mocek, K.; Klementova, M.; Carbonne, D. *Chem. Mater.* **2008**, *20*, 2985.